Electronic states of the pristine and alkali-metal-intercalated monolayer graphite/Ni(111) systems

A. Nagashima, N. Tejima, and C. Oshima
Department of Applied Physics, Waseda University, 3-4-1 Okubo, Shinjuku-ku, Tokyo 169, Japan
(Received 28 July 1994)

The electronic states of the pristine and alkali-metal-intercalated monolayer graphite (MG)/Ni(111) systems are investigated by using angle-resolved ultraviolet photoelectron spectroscopy and x-ray-photoelectron spectroscopy (XPS). The electronic structure of the MG is modified largely by hybridization of the π orbitals of the graphite layer with the d orbitals of the substrate. The deposition of alkali-metal atoms onto the graphite overlayer at room temperature results in the penetration of the adsorbates into the interface between the MG and the Ni(111) surface. This intercalation causes the change in the band structure of the system because of the dilation of the MG-Ni interlayer distance. The intercalation of the alkali-metal atoms also shows the broadening of the XPS peak of the C 1s core level of the MG.

I. INTRODUCTION

The behavior of carbon overlayers on transition-metal (TM) surfaces has been of great interest for a long time in relation to catalysis.[1-13] There exist two distinct states of carbon adatoms which are termed "carbidic" and "graphitic," respectively. While the carbidic carbon is active for CO methanation, the graphitic one is inactive.[1-4] The graphitic carbons on the surfaces of the TM and transition-metal carbide (TMC) are known to form monolayer graphite (MG).[8,11,14-18] This overlayer has long been considered to have almost identical properties with those of bulk graphite because of its anisotropic bond nature, which reflects the chemical inertness mentioned above.

From surface extended energy-loss fine-structure experiments, Rosei *et al.* have estimated the C-Ni distance of the MG/Ni(111) to be 3.1 Å, which is smaller than the interlayer C-C distance of the bulk graphite by ~ 0.3 Å.[8] Taking into account the larger radius of the Ni atom than that of the C atom, this result has suggested the strong bond between the MG and the Ni(111) surface in comparison with the weak interlayer bond in the bulk graphite. Nevertheless, from the results of angle-integrated ultraviolet photoelectron spectroscopy (AIUPS), Rosei *et al.* concluded that the interaction of the graphite overlayer with the metal substrate is very weak and shows up mainly as a charge transfer.[9] On the contrary, recent studies by using high-resolution electron-energy-loss spectroscopy have shown a large difference in the phonon dispersion between the bulk graphite and the MG, depending on the substrate.[16-18] On chemically reactive substrates such as (111) and (100) surfaces of Ni and (111) surfaces of the TMC's, the MG shows a large weakening of the in-plane C-C bond and the strengthening of the interplane bond compared to the corresponding bulk ones. In contrast to this, on relatively inert surfaces such as Pt(111) and the (100) surfaces of the TMC's, such changes in the bonds of the MG have not been observed.[17,18] These results indicate that the precise investigation of the electronic states of the graphite overlayer is indispensable for clarifying the nature of the bond between the MG and the metal substrate. For this purpose, the combination of *angle-resolved* UPS (ARUPS) and x-ray-photoelectron spectroscopy (XPS) is powerful, since it presents information on both the valence and core electrons. Especially, the ARUPS measurement enables one to acquire the dispersion relations of the valence bands, which is impossible with the AIUPS.

In this experiment, we have explored the electronic states of the pristine and alkali-metal-dosed MG/Ni(111) systems by using ARUPS and XPS. Electronic structure of the MG is changed strongly from that of the bulk graphite by hybridization of the π orbitals of the graphite layer with the d orbitals of the substrate. This is different from the case of alkali-metal graphite intercalation compounds (AGIC's), of which the band structure is changed by the electron transfer from the intercalants to the graphite layer.[19] The absence of such charge transfer in the MG/Ni(111) system seems reasonable since the electronegativity of the Ni atom (1.7) is larger than those of the alkali-metal atoms (~ 0.8). Here, an additional question may arise in connection with this result; when the alkali-metal atoms are deposited onto the MG, do they interact with the graphite overlayer via charge transfer, i.e., do they serve as a donor similar to the case of the AGIC's? This was the first motivation to undertake the study of the alkali-metal-adsorbed MG/Ni(111) system. In contrast to such simple expectation, however, the adsorbed alkali-metal atoms were found to behave in a complicated way. The alkali-metal atoms penetrate under the MG at room temperature and dilate the interlayer distance between the graphite overlayer and the substrate, which introduces the weakening of the interlayer bond. In addition, we have observed the large broadening of the XPS peak; the C 1s peak of the MG has become very broad and asymmetric upon the intercalation of the alkali-metal atoms. This phenomenon is attributed to the s electrons of the alkali-metal atoms which screen the potential of the C 1s core hole.

0163-1829/94/50(23)/17487(9)/$06.00

II. EXPERIMENT

The experiments were done in an ultrahigh vacuum (UHV) chamber equipped with a low-energy-electron-diffraction (LEED) optics, a gas inlet, a hemispherical energy analyzer, an ultraviolet discharge lamp, and an x-ray source. The unpolarized He I ($h\nu=21.2$ eV) and He II (40.8 eV) resonance lines were used for ARUPS and the characteristic x-rays of Mg $K\alpha$ (1253.6 eV) and Al $K\alpha$ (1486.6 eV) were used for XPS. For the UPS and XPS measurements, the analyzer was set to have the resolution of 0.2 and 0.5 eV, respectively. Since the linewidths of the Mg $K\alpha$ and Al $K\alpha$ x rays are 0.7 and 0.8 eV, the overall energy resolution for the XPS measurements was about 0.9 ± 0.04 eV. The base pressure in the vacuum chamber was $\sim 1\times10^{-8}$ Pa. The substrate used in this experiment was a Ni(111) surface. One face of the specimen was mechanically polished and chemically etched. In the UHV chamber the specimen was further cleaned by repeated cycles of Ar-ion sputtering and annealing at about 800 °C. After these procedures, the LEED pattern of the clean surface showed sharp diffraction spots in a low background, corresponding to a 1×1 atomic structure. No impurities such as oxygen or carbon were detected in the XPS spectra.

The graphite overlayer was grown epitaxially by dissociation of ethylene gas on the substrate at high temperature (≥ 600 °C). The graphite layer grown on the substrate at lower temperature (≤ 500 °C) had worse crystalline quality than that prepared at higher temperature, which was manifested in the LEED pattern and ARUPS spectra. The growth of the graphite layer is automatically stopped when the substrate is covered completely with the monolayer graphite. This is related to the fact that the surface reactivity for ethylene dissociation is strongly reduced by the formation of the graphite overlayer. To form a monolayer graphite, an exposure to ethylene gas of a few hundred langmuir (1 L $=1\times10^{-6}$ Torr s) was necessary. After this preparation, a C 1s peak appeared in a XPS spectrum at the binding energy of ~ 285 eV (as discussed later in Fig. 7), indicating the existence of the graphitic carbon. A sharp (1×1) LEED pattern of the sample showed the commensurate relation between the overlayer and the Ni(111) surface, which would be of great advantage to the theorists in performing calculations of this system since the other substrates have incommensurate relations with the MG.

Alkali-metal atoms (Cs, K, and Na) were dosed onto the clean and graphite-covered Ni(111) surfaces at room temperatures from a commercial SAES getter sources which had been carefully degassed. The background pressure rise in the chamber during evaporation was less than 2×10^{-8} Pa. Every three hours after the deposition, the alkali-metal-adsorbed MG/Ni(111) system was cleaned by annealing at the temperature over 400 °C, and alkali-metal atoms were deposited again onto the surface to make up for the desorbed ones. The amount of adsorbed atoms was checked with XPS. For the Cs adsorption onto MG/Ni(111), only a (2×2) LEED pattern was observed as an ordered adsorbate structure. After the formation of this superstructure, the sticking probability of Cs atoms onto the sample surface becomes extremely small and further adsorption brings the increase in the background in the LEED pattern. Corresponding superstructure for the K and Na adsorption were $(\sqrt{3}\times\sqrt{3})R30°$ and $(\frac{3}{2}\times\frac{3}{2})$, respectively. Hereafter, we call the coverage of adsorbed atoms necessary to form these superstructure "saturation coverage." In this paper, we concentrate our discussion mainly upon a pristine MG/Ni(111) system and alkali-metal-adsorbed MG/Ni(111) systems at the saturation coverages.

III. RESULTS AND DISCUSSION

A. Band structure of clean graphite overlayer

Figures 1(a) and 1(b) show typical ARUPS spectra of the clean MG/Ni(111) obtained for the $\bar{\Gamma}\bar{K}$ direction of the two-dimensional Brillouin zone excited by He I and He II resonance lines, respectively. Emission angle referred to the surface normal is denoted for each spectrum. In Fig. 1, there are some dispersionless peaks near E_F. As discussed later, they are mainly due to the metal d bands of the substrate, although the graphite overlayer is also related to these peaks. Besides these peaks, there are some other peaks in Fig. 1, which indicate large energy dispersions. Since none of them has been observed for clean substrate, they are all related to electronic states either in the MG or at the interface.

In Fig. 2, we plotted the binding energies (E_B) of the observed peaks in the ARUPS spectra of the MG/Ni(111) versus the wave vector parallel to the surface ($k_\parallel$) obtained by using the following formula:

$$k_\parallel=[2m(h\nu-\phi-E_B)/\hbar^2]^{1/2}\sin\theta\ , \tag{1}$$

where m is the rest mass of an electron, $h\nu$ the photon energy for excitation, ϕ the work function of the MG (3.9 eV, determined in the present study), and θ the emission angle relative to the surface normal. Open and solid circles represent the data obtained with He I and He II resonance lines, respectively. The corresponding energy bands of the graphite crystal are also indicated by broken curves.[20] In Fig. 2, there is one branch along the $\bar{\Gamma}\bar{K}$ with a steep energy dispersion in the energy region of 7–9 eV, which was observed only with He I. In the previous work,[21] we have assigned this branch to the secondary electron peaks, which show the dispersion relation of a conduction band in the MG.

The observed band structure of the MG is different from that of the graphite crystal indicated by broken curves in Fig. 2; while the σ bands of the MG agree with those of the bulk graphite fairly well, the π band differs remarkably from the bulk one in the following two features. First, the π band of the MG lies in the much deeper binding energy than the bulk one does. The binding energy of the π band at the $\bar{\Gamma}$ point is 10.3 eV, which is larger than the bulk value by about 2.2 eV. Second, in the bulk graphite, the π band reaches E_F at the K point of the Brillouin zone and connects with the unoccupied π^* band there.[22] As for the MG, on the other hand, such a conduction band connected with the π band was not observed around the $\bar{K}$ point. As shown in Fig. 2, one

branch was detected in the second Brillouin zone, which was connected with the π band at the $\bar{K}$ point. This could be a vestige of the severely deformed π^* band.

The origin of the observed difference in the band structure is discussed below. In the AGIC's, electrons are donated from the intercalants to the graphite layer, which causes a rise of the chemical potential (i.e., E_F) of the graphite. Consequently, all the valence bands of the graphite layer are shifted almost rigidly toward higher binding energies.[19] If this so-called "rigid-band model" is also valid for the MG and the observed difference in the energy of the π band between the MG and the bulk graphite is caused by electron transfer from the substrate to the MG, the σ bands should also have shifted to much deeper binding energy. However, the energy difference of the σ bands between the MG and the bulk is fairly small. Therefore, the rigid-band model is not valid for the energy band structure of the MG. Instead, from the fact that only the π and π^* bands are deformed severely from the bulk ones, mixing of the π/π^* states with the metal d states of the substrate are suggested.

The above interpretation is strongly supported by comparing the energies of the d bands before and after the formation of the MG. In Fig. 2, hatched bands with horizontal lines indicate the dispersion relations of the d bands of the clean Ni(111) surface observed with He I. Although some branches of the clean Ni(111) agree well with those of the MG-covered Ni(111), some other branches are different in energies from the corresponding ones of the MG/Ni(111) system or they do not have the corresponding ones at all. Therefore, we conclude that the hybridization between the π orbitals of the MG and the d orbitals of the Ni(111) surface causes the observed

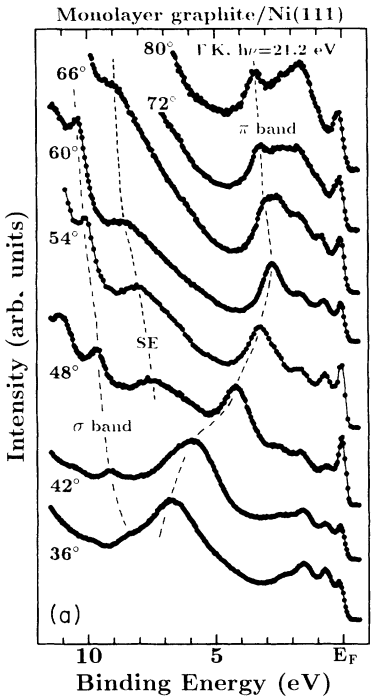

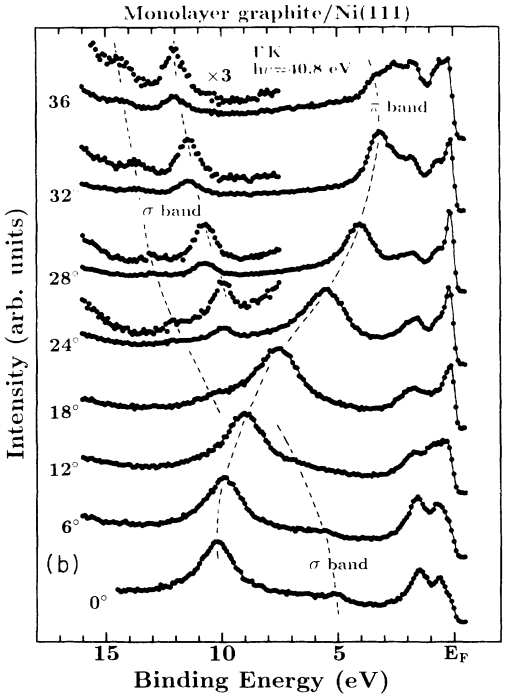

FIG. 1. Typical ARUPS spectra of the MG/Ni(111) excited by (a) He I ($h\nu$=21.2 eV) and (b) He II (40.8 eV), respectively. The polar angle of emitted electrons is denoted for each spectrum. "SE" is an abbreviation for "secondary electron."

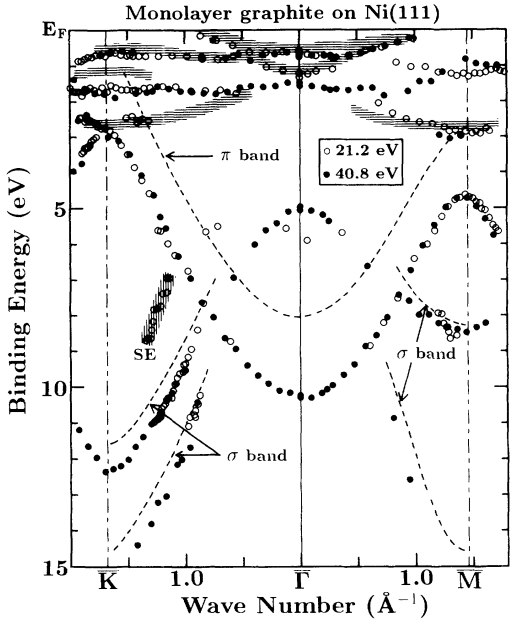

FIG. 2. Experimental band structure of the MG/Ni(111). Open (filled) circles denote the data obtained with He I (He II) resonance line. Shaded bands with horizontal lines near E_F indicate the dispersion relations of the d bands for the clean Ni(111) surface measured with He I. Experimental dispersion of the bulk graphite (Ref. 20) are also indicated by broken curves for comparison. SE is an abbreviation for secondary electron.

band-structure change.

This orbital hybridization also leads to the weakening of the in-plane C-C bond in the following way. The mixing of the occupied π states with the unoccupied substrate states causes the reduction of the occupation in the π states. On the other hand, the occupation of the unoccupied, antibonding π^* states increases due to the mixing with the occupied substrate states, which results in the weakening of the bond in the graphite layer. In other words, the bond weakening is caused by the electron redistribution from the bonding π states to the antibonding π^* states, of which the energies are lowered by the mixing with the substrate states. This is very different from the case of the AGIC's, in which the bond weakening is caused by the electron transfer from the intercalants into the unoccupied π^* band.[23] A mechanism similar to the present one was deduced from the theoretical and experimental studies of the electronic structure of the MG formed on the (111) surfaces of the TMC's.[21,24,25]

B. Intercalation of adsorbed atoms

In order to investigate the adsorbed positions of alkali-metal atoms relative to the graphite layer, angle-resolved XPS (ARXPS) measurements were carried out for the alkali-metal-adsorbed MG/Ni(111) systems at the saturation coverages, immediately after the deposition. Figure 3 shows the intensity ratios of the core-level peak of the carbon atoms in the MG to those of the alkali-metal atoms as a function of the emission angle θ referred to the surface normal. In Fig. 3, the normalized value of $R(\theta)/R(85°)$ is plotted for convenience sake, where $R(\theta)$ is a peak intensity ratio at θ. For the Cs-, K-, and Na-adsorbed MG/Ni(111) systems, the observed value of $R(85°)$ were 0.96, 2.33, and 0.81, respectively. As shown in Fig. 3, the relative intensity of the C 1s peak increases steeply as the emission angle gets closer to the grazing angle. This tendency suggests that the adsorbed alkali-metal atoms have penetrated under the graphite layer, as illustrated in Fig. 4.

A similar phenomenon has been also reported for the MG on the (111) and (100) surfaces of Ir.[26] In these systems, K, Cs, Ba, Pt, and Si atoms readily penetrate under the MG and reside between the graphite overlayer and the Ir substrate. Tontegode has attributed the mechanism for the intercalation to a thermal excitation of an edge atom of the graphite island; with an excess kinetic energy, this edge atom may break its bond with the Ir surface and also the bonds of several neighboring atoms of the graphite layer with this surface. Such a "carbon hole" enables the adsorbed atoms to migrate to the region beneath the layer.[27] In addition, from the LEED observation and intensity analysis, Wu and Ignatiev have pointed out the necessity of surface steps for the intercalation of K atoms between the layers of the bulk graphite.[28] Therefore, we conclude that for the present MG/Ni(111) system, adsorbed alkali-metal atoms penetrate under the graphite layer through defects and reside between the MG and the Ni(111) surface.

C. Band-structure change induced by intercalation

Figures 5(a) and 5(b) show typical ARUPS spectra of the Cs-adsorbed MG/Ni(111) system at the saturation coverage measured along the $\bar{\Gamma}\bar{K}$ symmetry axis. In Fig. 5(b), a Cs 5p core-level peak was weakly observed at the binding energy of ~ 11.5 eV at normal emission. With the increase of the emission angle, this peak has disap-

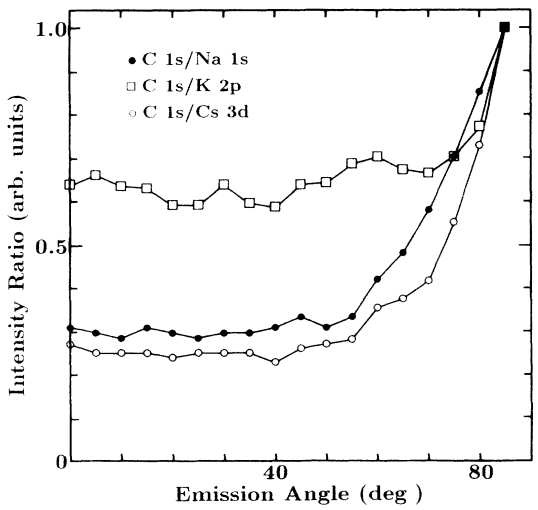

FIG. 3. The relative intensities of the XPS core-level peak for the MG to those for the adsorbed alkali-metal atoms as a function of the emission angle θ referred to the surface normal. In this figure, the normalized value of $R(\theta)/R(85°)$ is plotted for convenience sake, where $R(\theta)$ is an intensity ratio at θ. For the Cs-, K-, and Na-adsorbed MG/Ni(111) systems, the observed values of $R(85°)$ were 0.96, 2.33, and 0.81, respectively.

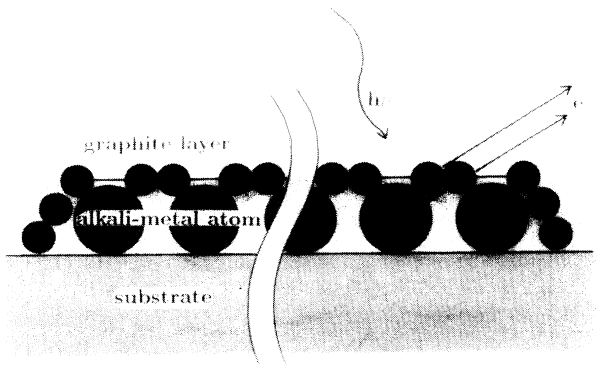

FIG. 4. A schematic picture of the relative position among the graphite overlayer, alkali-metal atoms adsorbed onto the MG/Ni(111) system, and the Ni(111) surface. The alkali-metal atoms penetrate under the graphite layer and reside between the MG and the substrate. The relative intensity of the core-level peak for the alkali-metal atoms to that for the carbon atoms decreases with the increase of the emission angle because of the finite mean free path of the photoelectrons.

peared. In addition, as shown in Figs. 1(b) and 5(b), the relative intensities of the substrate peaks near E_F to the π peak become small upon the Cs adsorption; this tendency was observed also for the K- and Na-adsorbed MG/Ni(111) systems. These results confirm the above conclusion deduced from the ARXPS measurement that the alkali-metal atoms have been intercalated between the graphite layer and the substrate.

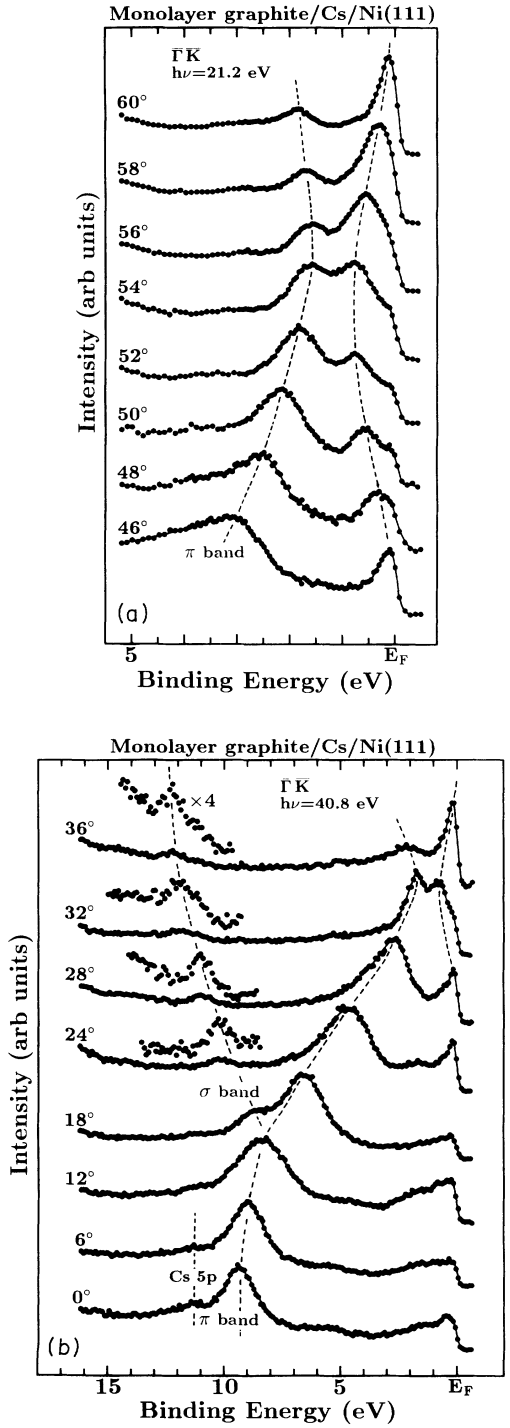

FIG. 5. Typical ARUPS spectra of the Cs-intercalated MG/Ni(111) system at the saturation coverage, which are excited by (a) He I and (b) He II resonance lines, respectively.

The series of peaks located at 0–1 eV in Figs. 5(a) and 5(b) manifest the metallic character of the overlayer. The binding energies of these peaks cross E_F, which presents a striking contrast to the semimetallic character of the bulk graphite. It should be remarked that such peaks are not observed for the clean MG/Ni(111) system. Figure 6(a) shows the band structure of the Cs-dosed MG/Ni(111) system. Although the observed dispersion relation of the metallic peak around the $\bar{K}$ point is similar in shape to that of the π^* band in the bulk graphite,[22] there is a band gap of 0.7 eV at the $\bar{K}$ point between the conduction band and the π band. This result signifies that the simple rigid band model accompanied with the electron transfer from the intercalants and/or the substrate to the graphite layer is not valid for the Cs-adsorbed MG on Ni(111) surface.

As shown in Figs. 2 and 6(a), the π band has shifted toward shallower binding energy upon the Cs adsorption, while the energy shifts of the σ bands were very small. This is notably different from the case of the AGIC's, where *all* the valence bands are shifted to *deeper* binding energies by the electron transfer from the intercalants to the graphite layer.[19] On the contrary, the band structure of the MG has become very similar to that of the bulk graphite upon the Cs adsorption; the difference in the energy of the π band between the MG and the bulk graphite has become small, and the π^*-like conduction band has appeared around the $\bar{K}$ point, which was not observed for the pristine MG/Ni(111).

Figures 6(b) and 6(c) show the band structures of the K- and Na-adsorbed MG/Ni(111) systems at the saturation coverages, respectively. The ARUPS spectra of these systems (not shown) are quite similar in shape to those of the Cs-adsorbed system shown in Fig. 5, and the band structures of the three systems are also very similar to each other. However, there is a rather small but clear difference among these systems. In Table I, we tabulate the observed binding energies of the π band at the $\bar{\Gamma}$ point and the band-gap energies at the $\bar{K}$ point between the π and π^*-like bands. The coverages of the adsorbed alkali-metal atoms are also indicated in Table I, where the coverage Θ is defined as the number of alkali-metal atoms per surface Ni atoms. In view of the fact that for

TABLE I. The observed binding energies of the π band at the $\bar{\Gamma}$ point and the band-gap energies between the π band and the π^*-like conduction band at the $\bar{K}$ point are tabulated. Coverages of the alkali-metal atoms are also indicated.

Sample	Binding energy of π band at $\bar{\Gamma}$ (eV)	Band gap at $\bar{K}$ (eV)	Coverage
MG/Ni(111)	10.3		
MG/Na/Ni(111)	9.7	1.3	0.45
MG/K/Ni(111)	9.6	0.8	0.34
MG/Cs/Ni(111)	9.3	0.7	0.25

the AGIC's, the degree of the change in the band structure and the bond strength is ruled mainly by the amount of transferred charge from the intercalants to the graphite layer (i.e., amount of alkali atoms) but not by the species of the adsorbate,[19,23] it may well be supposed that a similar dependence on the coverage could be observed in the present alkali-metal-adsorbed MG. However, it is clearly seen in Fig. 6 and Table I that with the increase of the radius of the absorbed atoms, the band structure of the graphite overlayer changes to a larger extent and gets closer to the bulk one, regardless of the decrease in the coverage Θ; the π band shifts to the lower binding energy approaching the bulk value and the band gap decreases. These experimental facts indeed confirm our conclusion discussed in the previous section that the absorbed atoms reside between the MG and the Ni(111) surface. The intercalation of the alkali-metal atoms between the MG and the Ni(111) surface causes the dilation of the interlayer distance, which weakens the interlayer bond. As a consequence, the band structure of the MG becomes

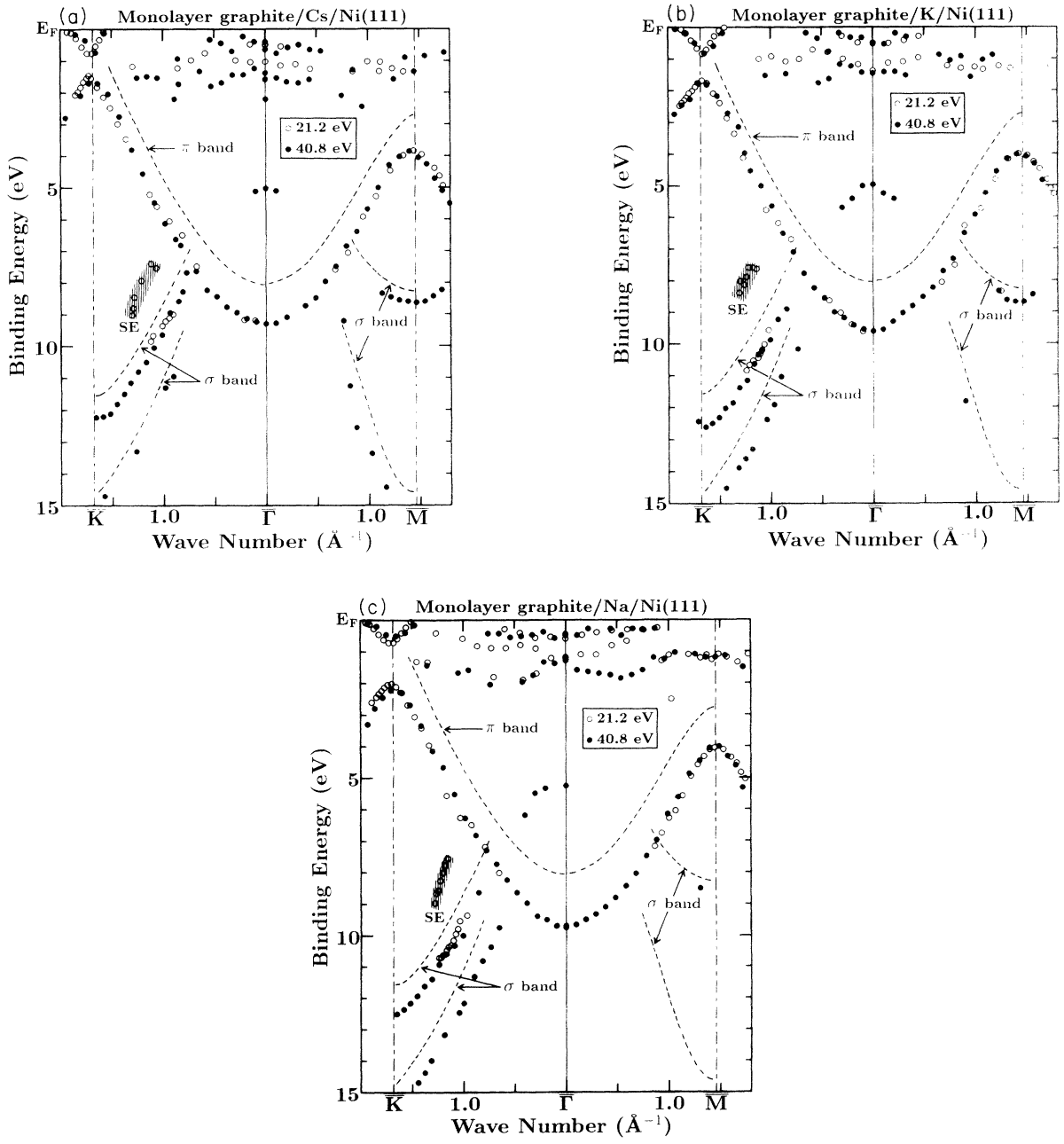

FIG. 6. Experimental band structure of the alkali-metal-intercalated MG/Ni(111) systems with (a) Cs, (b) K, and (c) Na atoms at the saturation coverages, respectively.

TABLE II. Work function of the pristine and alkali-metal-intercalated MG/Ni(111) systems.

Sample	Work function (eV)
MG/Ni(111)	3.9
MG/Na/Ni(111)	3.0
MG/K/Ni(111)	2.9
MG/Cs/Ni(111)	3.0

similar to the bulk one depending on the radius of the intercalants.

Table II shows the work function of the pristine and alkali-metal intercalated MG/Ni(111) systems. The present work function change, $\Delta\phi \sim -1$ eV is much smaller in magnitude than that induced by the alkali adsorption onto the clean Ni(111) surface at the "saturation" coverage ($\Delta\phi \leq -2$ eV).[29] In addition, the work functions of the three intercalated systems are almost the same, which is different from the case of the alkali adsorption onto metal surfaces, where the degree of the work-function change depends on the adsorbate.[30] This result suggests that the electron distributions in the outermost graphite layer of the three systems are similar to each other, and that the charge redistribution occurs mainly between the alkali-metal atoms and the substrate but not between the alkali-metal atoms and the graphite layer. On the other hand, the observed energies of the XPS core-level peak of the alkali-metal atoms adsorbed onto the clean and graphite-covered Ni(111) surfaces were almost identical with each other. This fact implies that the alkali-metal atoms in each of these two systems have a similar electron distribution. Therefore, it could be inferred that in the intercalated MG/Ni(111) system, the charge redistribution occurs not only between the alkali-metal atoms and the substrate but also within the graphite layer itself, which results in the smaller work function change.

The observed change in the band structure and the work function brought about by the intercalation indicates that the intercalants are reluctant to donate electrons to the graphite overlayer compared to the case of the AGIC's, in which the alkali-metal atoms donate their valence electrons almost completely to the graphite host.[23] This might be related to the fact that the alkali-metal adatoms on metal substrates are essentially neutral, at least, in the high coverage region, and the charge redistribution occurs within the atomic sphere.[31] In other words, it seems suitable for the first-order approximation to regard the intercalated MG/Ni(111) system as the weakly perturbed MG in contact with the alkali-metal-overlayer/Ni(111) system.

D. Line broadening of C 1s peak

Figure 7 shows the XPS spectra in the C 1s energy region for the pristine and intercalated MG and for the bulk graphite obtained with Mg $K\alpha$ line. Roughly speaking, the C 1s peak of the clean MG/Ni(111) is very similar in shape to that of the bulk graphite, although the small energy shift to the higher binding energy is observed. The absence of large chemical shift to *lower* binding energy manifests that the electron transfer from the substrate to the graphite layer is, if any, small.

The C 1s line shapes of the intercalated MG/Ni(111) systems are quite different from those of the pristine MG/Ni(111) and the bulk graphite. The full width at half maximum has increased drastically from 1.3 eV for the pristine MG to 2.0–2.2 eV for the intercalated MG, whereas the energy position of the C 1s line stays almost unchanged. Furthermore, the C 1s peak of the intercalated MG is very asymmetric compared to that of the pristine MG. In Fig. 7, we also depicted the difference spectra just under the original spectra of the intercalated MG/Ni(111) systems. They are calculated by subtracting the spectrum of the pristine MG from those of the intercalated systems; the intensities of the original spectra were adjusted in order not to make any artificial structures in the difference spectra. It is clearly seen from Fig. 7 that the intercalated systems have an additional structure at the deeper binding energy, which departs from the main C 1s line by ~0.8 eV.

A similar broadening of the C 1s line was reported for the Li-intercalated graphite compounds (LiC_6), and it was tentatively ascribed to the surface carbon atoms

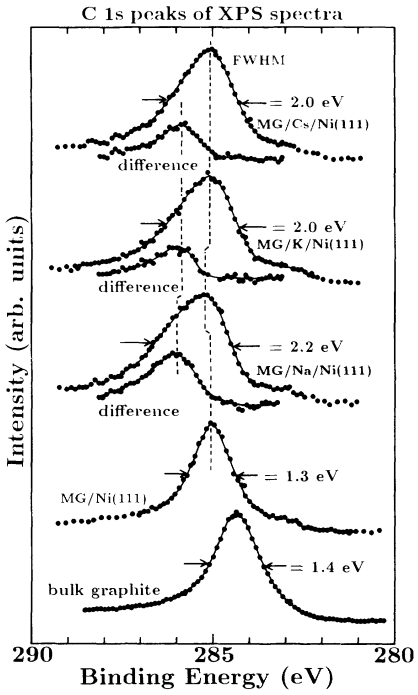

FIG. 7. C 1s region of XPS spectra of the clean and alkali-metal-intercalated MG/Ni(111) systems. The XPS spectrum of the bulk graphite is also indicated for comparison. The difference spectra were calculated by subtracting the original spectra of the pristine MG from those of the intercalated systems. The value of the full width at the half maximum of the C 1s peak is indicated for each spectrum.

which do not have the full Li neighbor environment.[32] Such explanation is not applicable to the alkali-metal-intercalated MG/Ni(111) system, because of the monolayer thickness of the graphite overlayer. A possible mechanism for the line broadening in the present system is discussed below. Since the adsorbed alkali-metal atoms form the superstructures, the positions of the neighboring carbon atoms in the graphite layer may not be identical with each other, which is exactly true especially for the (2×2) and $(\frac{3}{2}\times\frac{3}{2})$ superstructures. From this difference in position, one might expect the following effects: the carbon atoms nearer the alkali-metal atoms would be donated more electrons from the intercalants than the farther carbon atoms and the core holes created in the nearer atoms would be screened more effectively. However, such expectation can be discarded, since it would introduce an asymmetry to lower binding energy and, moreover, it contradicts the small electron transfer discussed in the previous section. Instead, the observed asymmetry to the higher binding energy signifies that the energy loss occurs in the photoemission process. It should be noted that the line broadening of the Ni $2p$ core-level peak was not induced upon the intercalation of the alkali-metal atoms, i.e., no difference was detected in the shape of the Ni $2p$ peak between the pristine and intercalated MG/Ni(111) systems. This fact strongly suggests that the energy-loss process is of intrinsic (i.e., core-hole-induced) character rather than the extrinsic (photoelectron-induced) one for the removal of the electron from the C $1s$ state. In addition, from the fact that the C $1s$ line broadening occurs only in the intercalated MG/Ni(111) systems but not in the pristine MG/Ni(111), one could recognize the important role of the s electrons of the alkali-metal atoms which screen the C $1s$ core hole. Therefore, the line broadening is ascribed to many-body effects involving the energy loss for the excitation such as the plasmon or interband transition, with which the s electrons of the alkali-metal atoms are concerned. The similar broadening was reported for the O $1s$ and C $1s$ peaks of the CO chemisorbed on the Ni(111) surface; in this system, the screening electrons occupy the CO $2\pi^*$-derived resonance states, of which the energies are lowered by the sudden creation of the core hole.[33]

IV. CONCLUSIONS

By using angle-resolved UPS and XPS, we have investigated the electronic and structural properties of the pristine and alkali-metal-intercalated MG/Ni(111) systems. The electronic structure of the MG is modified strongly from that of the bulk graphite by the mixing of the π/π^* states of the graphite layer with the d states of the substrate. This is very different from the case of the AGIC's, where the electron transfer from the intercalants to the graphite layer causes the band-structure change. The adsorbed alkali-metal atoms (Cs, K, and Na) penetrate into the interface between the MG and the substrate at room temperature, dilating the interlayer distance, which causes the weakening of the interlayer bond. As a consequence, the band structure of the intercalated MG becomes very similar to that of the bulk graphite depending on the radius of the intercalants. In energetic point of view, these results indicate that the intercalation of the alkali-metal atoms between the MG and the Ni(111) surface is favorable, nevertheless it involves the weakening of the bond between the graphite overlayer and the substrate. In addition, the XPS peak of the C $1s$ core level of the MG becomes very broad and asymmetric upon the intercalation. This phenomenon is attributed to the energy-loss process, to which the s electrons of the alkali-metal atoms are related.

ACKNOWLEDGMENTS

We are grateful to Professor M. Tsukada of University of Tokyo for his valuable comments. One of the authors (A.N.) was supported by the Japan Society for the Promotion of Science.

[1]M. Eizenberg and J. M. Blakely, Surf. Sci. **82**, 228 (1979).
[2]D. W. Goodman, R. D. Kelley, T. E. Madey, and J. T. Yates, Jr., J. Catal. **63**, 226 (1980).
[3]H. L. Bonzel and J. H. Krebs, Surf. Sci. **91**, 499 (1980).
[4]P. J. Feibelman, Surf. Sci. **103**, L149 (1981).
[5]F. J. Himpsel, K. Christmann, P. Heimann, D. E. Eastman, and P. J. Feibelman, Surf. Sci. **115**, L159 (1982).
[6]P. J. Feibelman, Phys. Rev. B **26**, 5347 (1982).
[7]K. Yamamoto, M. Fukushima, T. Osaka, and C. Oshima, Phys. Rev. B **45**, 11 358 (1992).
[8]R. Rosei, M. De Crescenzi, F. Sette, C. Quaresima, A. Savoia, and P. Perfetti, Phys. Rev. B **28**, 1161 (1983).
[9]R. Rosei, S. Modesti, F. Sette, C. Quaresima, A. Savoia, and P. Perfetti, Phys. Rev. B **29**, 3416 (1984).
[10]L. Papagno and L. S. Caputi, Phys. Rev. B **29**, 1483 (1984).
[11]E. V. Rut'kov and A. Y. Tontegode, Surf. Sci. **161**, 373 (1985).
[12]C. F. McConville, D. P. Woodruff, and S. D. Kevan, Surf. Sci. **171**, L4417 (1986).
[13]J. Nakamura, I. Toyoshima, and K. Tanaka, Surf. Sci. **201**, 185 (1988).
[14]H. Itoh, T. Ichinose, C. Oshima, T. Ichinokawa, and T. Aizawa, Surf. Sci. **254**, L437 (1991).
[15]T. A. Land, T. Michely, R. J. Behm, J. C. Hemminger, and G. Comsa, Surf. Sci. **264**, 261 (1992); J. Chem. Phys. **97**, 6774 (1992).
[16]T. Aizawa, R. Souda, Y. Ishizawa, H. Hirano, T. Yamada, K. Tanaka, and C. Oshima, Surf. Sci. **237**, 194 (1990).
[17]T. Aizawa, Y. Hwang, W. Hayami, R. Souda, S. Otani, and Y. Ishizawa, Surf. Sci. **260**, 311 (1992).
[18]T. Aizawa, R. Souda, S. Otani, Y. Ishizawa, and C. Oshima, Phys. Rev. Lett. **64**, 768 (1990); Phys. Rev. B **42**, 11 469 (1990); Y. Hwang, T. Aizawa, W. Hayami, S. Otani, Y. Ishizawa, and S. J. Park, Surf. Sci. **271**, 299 (1992).
[19]F. P. DiVencenzo and S. Rabii, Phys. Rev. B **25**, 4110 (1982); N. A. W. Holzwarth, S. G. Louie, and S. Rabii, *ibid.* **28**, 1013 (1983); S. Mizuno, H. Hiramoto, and K. Nakao, Solid State Commun. **63**, 705 (1987); W. Eberhardt, I. T. McGovern, E. W. Plummer, and J. E. Fisher, Phys. Rev. Lett. **44**, 200 (1980); T. Takahashi, N. Gunasekara, T. Sagawa, and H. Suematsu, J. Phys. Soc. Jpn. **55**, 3498 (1986); N. Gunasekara,

T. Takahashi, F. Maeda, T. Sagawa, and H. Suematsu, *ibid.* **56**, 2581 (1987).

[20]T. Takahashi, H. Tokailin, and T. Sagawa, Phys. Rev. B **32**, 8317 (1985).

[21]A. Ngashima, H. Itoh, T. Ichinokawa, C. Oshima, and S. Otani, Phys. Rev. B **50**, 4756 (1994).

[22]R. C. Tartar and S. Rabii, Phys. Rev. B **25**, 4126 (1982).

[23]C. T. Chan, W. A. Kamitakahara, K. M. Ho, and P. C. Ecklund, Phys. Rev. Lett. **58**, 1528 (1987); C. T. Chan, K. M. Ho, and W. A. Kamitakahara, Phys. Rev. B **36**, 3499 (1987).

[24]K. Kobayashi and M. Tsukada, Phys. Rev. B **49**, 7660 (1994).

[25]A. Nagashima, K. Nuka, K. Sato, H. Itoh, T. Ichinokawa, C. Oshima, and S. Otani, Surf. Sci. **291**, 93 (1993).

[26]E. V. Rut'kov and A. Ya. Tontegode, Pis'ma Zh. Tekh. Fiz. **7**, 1122 (1981) [Sov. Tech. Phys. Lett. **7**, 489 (1981)]; Zh. Tekh. Fiz. **52**, 921 (1982) [Sov. Phys. Tech. Phys. **27**, 589 (1982)]; N. A. Kholin, E. V. Rut'kov, and A. Ya. Tontegode, Surf. Sci. **139**, 155 (1984); N. R. Gall', S. N. Mikhailov, E. V. Rut'kov, and A. Ya. Tontegode, Poverkhonost' **12**, 14 (1986); N. R. Gall', E. V. Rut'kov, and A. Ya. Tontegode, Pis'ma Zh. Tekh. Fiz. **14**, 527 (1988) [Sov. Tech. Phys. Lett. **14**, 235 (1988)].

[27]A. Ya. Tontegode, Pis'ma Zh. Tekh. Fiz. **15**, 57 (1989) [Sov. Tech. Phys. Lett. **15**, 271 (1989)].

[28]N. J. Wu and A. Ignatiev, Phys. Rev. B **28**, 7288 (1983).

[29]D. Tang and D. Heskett, Phys. Rev. B **47**, 10 695 (1993).

[30]S. Å. Lindgren and L. Walldén, Phys. Rev. B **22**, 5967 (1980).

[31]H. Ishida and K. Terakura, Phys. Rev. B **38**, 5752 (1988).

[32]G. K. Wertheim, P. M. Th. M. Van Attekum, and S. Basu, Solid State Commun. **33**, 1127 (1980).

[33]B. Gumhalter, Phys. Rev. B **33**, 5245 (1986); B. Gumhalter, K. Wandelt, and Ph. Avouris, *ibid.* **37**, 8048 (1988).

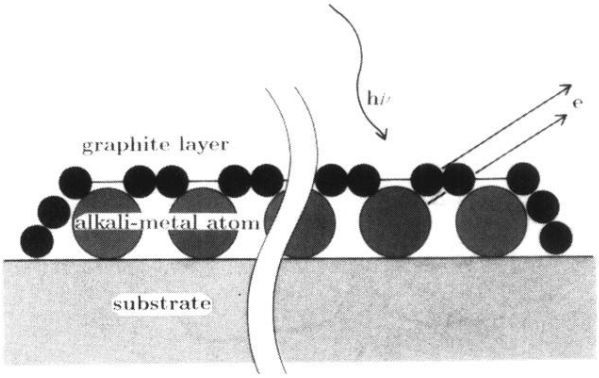

FIG. 4. A schematic picture of the relative position among the graphite overlayer, alkali-metal atoms adsorbed onto the MG/Ni(111) system, and the Ni(111) surface. The alkali-metal atoms penetrate under the graphite layer and reside between the MG and the substrate. The relative intensity of the core-level peak for the alkali-metal atoms to that for the carbon atoms decreases with the increase of the emission angle because of the finite mean free path of the photoelectrons.